Solid State Phenomena
ISSN: 1662-9779, Vol. 312, pp 113-120
doi:10.4028/www.scientific.net/SSP.312.113

Submitted: 2020-04-10
Revised: 2020-05-25
Accepted: 2020-05-26
Online: 2020-11-11

Au Nanoparticle-Decorated TiO_2 Nanospheres Produced by Laser Reshaping in Water

Stanislav Gurbatov[1,2,a*], Sergei Kulinich[2,3,b] and Aleksandr Kuchmizhak[1,2,c]

[1]Institute of Automation and Control Processes, Far Eastern Branch of the Russian Academy of Science, Vladivostok 690041, Russia

[2]Far Eastern Federal University, Vladivostok 690041, Russia

[3]Research Institute of Science and Technology, Tokai University, Hiratsuka, Kanagawa 259-1292, Japan

[a]gurbatov_slava@mail.ru, [b]skulinich@tokai-u.jp, [c]alex.iacp.dvo@mail.ru

Keywords: Hybrid nanomaterials, pulsed laser ablation in liquids, titanium dioxide

Abstract. Here, we demonstrate formation of spherical-shaped amorphous titania (TiO_2) nanoparticles decorated with Au nanoclusters via nanosecond pulse ablation (7-ns, 532-nm wavelength) of commercially available TiO_2 nanopowders dispersed in an aqueous solution of chloroauric acid ($HAuCl_4$). Generation of such hybrid nanostructures was found to be caused by laser-induced remelting of the initial TiO_2 nanoparticles, stimulated by Au nanoclusters that can adsorbed on their surface and boost light-to-heat conversion process in optically transparent titania. The morphology and chemical composition of the obtained hybrid nanomaterials were studied in detail via scanning electron microscopy, Raman spectroscopy and Energy Dispersive X-ray spectroscopy. The average size and number of Au nanoclusters reduced on the TiO_2 nanoparticle surface was shown to be tuned by varying the initial nanoparticles/$HAuCl_4$ concentration ratio. Spectroscopic measurements of single hybrid nanoparticles scattering, as well as the corresponding numerical calculations of electromagnetic fields structure near their surface indicate synthesized functional nanomaterials as extremely promising for numerous applications of modern optics, optoelectronics and nanophotonics, e.g., realization of advanced chemo- and biosensing platforms, as well as of new-generation solar cells.

Introduction

During the last three decades, studying the optical properties of metallic nanoparticles that support optically-induced resonance oscillations of their electron density (so-called 'localized plasmon resonance'), as well as highly-refractive submicron structures based on dielectrics and semiconductors, has been the mainstream of both fundamental and applied research in the fields of nanophotonics, plasmonics, and optoelectronics [1-4]. The continuous popularity of such nanomaterials is associated with their unique optical properties. In particular, plasmonic nanoparticles are known to generate multiply-enhanced electromagnetic fields (so-called 'hot spots') localized at subwavelength scale at their surface, while dielectric nanoparticles support optically-induced electrical and magnetic response (the Mie resonances), the latter providing both a significant field enhancement and the possibility to tune the directivity of radiation pattern, etc. [5,6]. It is therefore expected that combining both dielectric and plasmonic materials into a single hybrid resonant nanostructure will make it possible to produce a system with both controlled and tunable magnetic optical response, as well as with a high localization degree and enhancement of the electromagnetic field. Hence, this will permit to fabricate nanomaterials with unique optical properties, optimized ratio of radiation and non-radiation losses, and with an extended working wavelength range [7,8]. In particular, the hybrid nanostructures are prospective for beam steering, optical switching, generation of high harmonics, as well as for optical biosensors based on contact-free optical detection of surface-enhanced photoluminescence (SEPL), surface-enhanced Raman scattering (SERS) and surface-

enhanced infrared absorption (SEIRA) [9-12]. It should be noted that hybrid metal-dielectric nanomaterials are also actively studied in various photo- and electrocatalytic applications [13,14].

At the same time, the difference in sizes required of the semiconductor/dielectric nanoparticles and plasmonic nanoparticles (200-500 nm and <50 nm, respectively) to realize their simultaneous resonant response in the visible spectral range makes the production of such hybrid metal-dielectric nanostructures rather difficult and time-consuming, even if advanced and expensive lithography techniques are involved. The high-throughput wet-chemistry preparation can hardly be applied for fabrication of the hybrid nanostructures with precise control of optical properties, especially, based on high-index dielectric materials (Si, TiO_2, etc.) [15,16]. Furthermore, the utilization of various toxic substances during chemical synthesis of hybrid nanomaterials does not meet the growing requirements for the environmental friendliness.

Last year's show that pulsed laser ablation in liquids (PLAL) has proved to be a general and highly efficient technique to synthesize nanomaterials and fabricate functional nanostructures [17-20]. Compared with conventional nanomaterials production processes, such as gas-phase methods, which usually produce agglomerated micro- or nanopowders, and wet-chemistry methods, which generally provide nanomaterials with impurities originating from additives and precursor reaction products, pulsed laser ablation in liquids has the following advantages. PLAL is conducted under ambient conditions and does not require extreme temperature and/or pressure. PLAL is a chemically simple and clean because the process has little byproduct formation, simple starting materials, and no need for catalyst. These factors ensure production of highly pure clean surfaces that often possess high surface activity. Utilization of high-power laser irradiation involves both locally and temporally extreme conditions of temperature and pressure (and their gradients) that could not be attained otherwise, which allows one to produce nanomaterials with unique metastable phases [21-25]. Furthermore, the phase, size, and shape of nanostructures can be readily controlled by tuning laser parameters and assisting factors, allowing one-step fabrication of even complex nanostructures (core-shell, alloyed, decorated, hollow, cubic, etc.). However, only a few works concerning synthesis of dielectric nanomaterials decorated with plasmon nanoparticles via PLAL have been published [26–28]. Moreover, the prospects of using such hybrid nanomaterials in the nanophotonics applications are hardly discussed.

Here, we demonstrate formation of spherical-shaped amorphous titania (TiO_2) nanoparticles decorated with Au nanoclusters via nanosecond pulse ablation (7-ns, 532-nm wavelength) of commercially available TiO_2 nanopowders dispersed in an aqueous solution of chloroauric acid ($HAuCl_4$). Generation of such hybrid nanostructures was found to be caused by laser-induced remelting of the initial TiO_2 nanoparticles, stimulated by Au nanoclusters that can adsorbed on their surface and boost light-to-heat conversion process in optically transparent titania. The average size and number of Au nanoclusters reduced on the TiO_2 nanoparticle surface was shown to be tuned by varying the initial nanoparticles/$HAuCl_4$ concentration ratio. Spectroscopic measurements of single hybrid nanoparticles scattering, as well as the corresponding numerical calculations of electromagnetic fields structure near their surface indicate synthesized functional nanomaterials as extremely promising for numerous applications of modern optics, optoelectronics and nanophotonics, e.g., realization of advanced chemo- and biosensing platforms, as well as of new-generation solar cells.

Materials and Methods

To produce Au-decorated spherical TiO_2 nanoparticles, a commercially available TiO_2 nanopowder (anatase, Wako Chemicals, 99.99%) with an average particle size of 120 nm was used as a starting material (Fig. 1b). First, TiO_2 nanoparticles with a mass fraction of 0.001% were dispersed in deionized water under the influence of an ultrasonic homogenizer. Then, the suspension (7.5 ml) was transferred to a quartz cuvette (3 x 3 x 6 cm^3) and an aqueous solution of tetrachloroauric acid ($HAuCl_4$) with a concentration of 10^{-3} M was added (0.25 ml, 0.5 ml, 0.75 ml for various cases). After that, the suspension was irradiated with focused nanosecond laser pulses (Quantel Ultra 50, 7-ns, 532-nm wavelength, 20-Hz pulse repetition rate) for 2 hours (Fig. 1a).

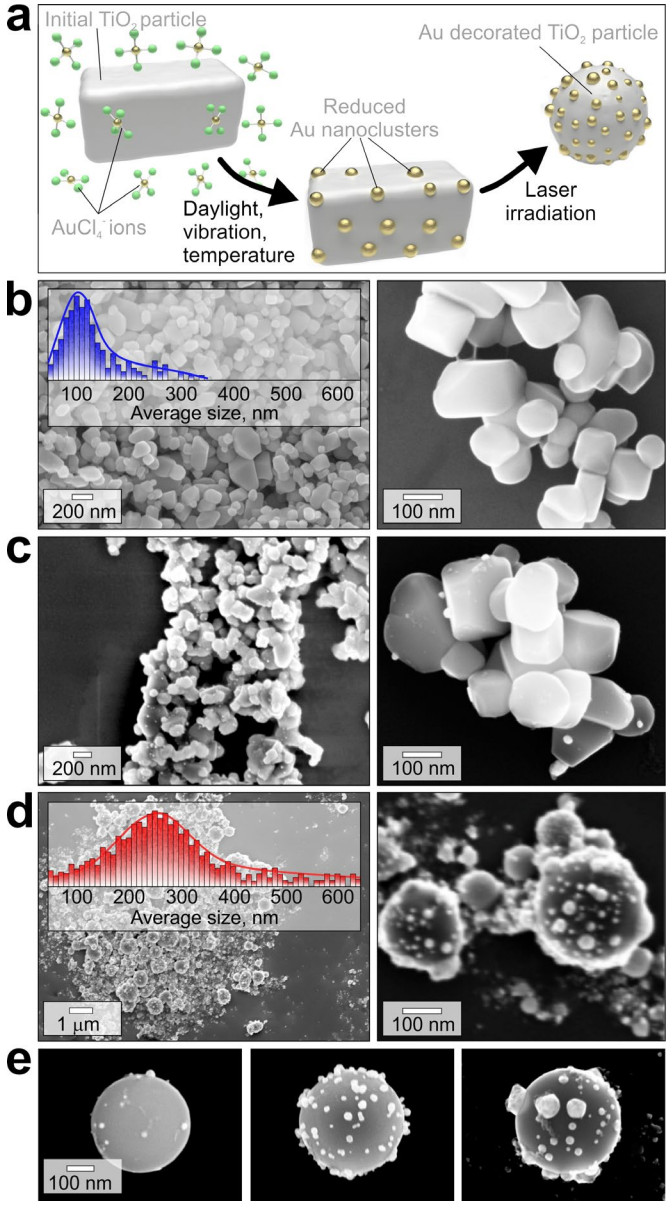

Fig.1 (a) Sketch showing consecutive steps behind formation of spherical-shaped Au-decorated TiO_2 nanoparticles. (b-d) SEM images of initial TiO_2 nanoparticles (b), similar nanoparticles aged for 2 h in a stirred aqueous solution of $HAuCl_4$ (c), Au-decorated TiO_2 nanoparticles after irradiation a suspension of the initial TiO_2 nanoparticles in an aqueous solution of $HAuCl_4$ (d). The right column represents enlarged SEM images of nanoparticles. Histograms of the nanoparticles size distributions before and after laser irradiation are shown in the insets (b,d). (e) SEM images of individual Au-decorated titania particles with tailored decoration produced at various initial $HAuCl_4$ concentration (10^{-4} M, $2x10^{-4}$ M, $3x10^{-4}$M, correspondingly).

The laser radiation energy was 25 mJ per pulse that was controlled by a power meter (Coherent FieldMaxII-TOP). The pulses were focused in the center of the cuvette by a lens with a 10-cm focal length. During irradiation, the suspension was constantly mixed with a 600-rpm magnetic stirrer. All laser irradiation experiments were performed under ambient environmental conditions at room temperature. After PLAL, the products dispersed in the liquid were collected, washed, and dialyzed carefully with deionized water to remove the remaining $HAuCl_4$ residues.

The morphology of nanomaterials obtained was characterized at all stages by high-resolution electron microscopy (Carl Zeiss, Ultra 55+). To do this, dispersed product (2.5-µl) was drop casted onto a crystalline silicon wafer and dried at a temperature of 70°C. Energy dispersive x-ray spectroscopy (EDX) was used to determine the chemical composition of hybrid nanoparticles. The crystalline phase of single nanoparticles was studied using Raman spectroscopy. To measure the

Raman spectra of synthesized nanoparticles, last were deposited on a silver mirror and then were pumped by stable semiconductor laser source (532-nm central wavelength, 50-W average power) focused on the sample surface by a dry objective lens with NA of 0.95. The Raman signal was collected by the same lens and analyzed using a grating spectrometer equipped with a cooled CCD camera (Andor Shamrock 303i and Andor Newton 935).

Optical resonances of the single hybrid nanoparticles were studied by confocal dark-field optical spectroscopy. The hybrid nanoparticles on glass substrate was excited at an oblique angle (70^o with respect to the normal of the surface) by p-polarized light from a supercontinuum generator through a weakly-focusing objective (10×, NA = 0.28). Scattered light was collected from the top by a 50× objective (NA = 0.95), and sent to a grating spectrometer equipped with a cooled CCD camera (Andor Shamrock 303i and Andor Newton 935). The structure and intensity of electromagnetic fields localized near hybrid Au-TiO_2 nanoparticles were studied by 3D finite-difference time domain (3D-FDTD) numerical simulations performed using a commercial software package (Lumerical Solutions).

Results and Discussion

SEM analysis of the initial TiO_2 nanopowder deposited on a silicon substrate showed that nanoparticles are of irregular shape and has an average size of ≈120 nm prior to irradiation with laser pulses (Fig. 1b). First of all, it should be noted that the initial nanoparticles themselves almost do not absorb 532-nm laser radiation used in present work. This is also evidenced by the fact that laser irradiation did not lead to any significant modification of nanoparticles shape and size without the addition of $HAuCl_4$ to the initial suspension. However, according to spectrophotometric studies (not shown in present work) the addition of $HAuCl_4$ does not change the absorption characteristics of the suspension at the specified wavelength. In our opinion, the above features indicate the key role of reduced on the titania surface gold nanoclusters in the laser-induced melting / modification of optically transparent TiO_2 nanoparticles. This is partially confirmed by the fact that the gold reduction on the initial particles surface can occur, for example, under the influence of daylight, ultrasound, vibration, etc. without laser irradiation. Identification the mechanism playing a key role is beyond the scope of this paper. Yet, we analyzed the morphology of the initial nanopowders (0.001%) dispersed in a 10^{-4}-M aqueous solution of $HAuCl_4$ and kept for 2 h in cuvette with magnetic stirrer, which is identical to the suspensions used later in PLAL experiments. SEM images clearly demonstrate the formation of gold nanoclusters with the average size of ≈15 nm on the initial TiO_2 nanoparticles (Fig. 1c). Irradiation of the specified suspensions with intense laser pulses for 2 h leads to Au-clusters-stimulated remelting of the irregular shaped nanomaterial into nanospheres with an average diameter of about 250 nm (Fig. 1d). Varying $HAuCl_4$ concentration in the solution allows one to tune the decoration degree (the number and average size of the deposited gold nanoparticles) of the hybrid nanomaterials obtained (Fig. 1e). Nucleation growth due to laser-induced photochemical reduction of the tetrachloroaurate complex $[AuCl_4]^-$ is believed to be the key mechanism for Au nanoparticles formation on TiO_2 nanospheres [29]. It is noteworthy that such an action results in all particles of the initial nanopowder to be converted into spherical nanoparticles. In this case, a shift in the average size of the obtained nanoparticles to higher values indicates that nanospheres can be formed by fusion of two or more nanoparticles. A series of similar experiments performed for various suspension irradiation times at fixed initial amount of $HAuCl_4$ showed that longer exposure (> 2 h) does not increase the decoration degree of TiO_2 particles, but leads to an increase in their average size and the emergence of microspheres with a diameter of up to 1.5 μm, which is appear to be caused by the secondary re-melting of TiO_2 particles. At a shorter irradiation time, unmodified nanoparticles were revealed in the obtained nanomaterials via SEM analysis.

EDX spectra of the starting and laser-irradiated nanomaterials demonstrate their only difference associated with the presence of characteristic gold peaks in the spectra of irradiated Au-TiO2 particles (Fig. 2a). At the same time, a comparison of the Raman spectra of hybrid nanoparticles with the starting nanomaterial exhibits a significant difference in their crystalline structure. All anatase peaks

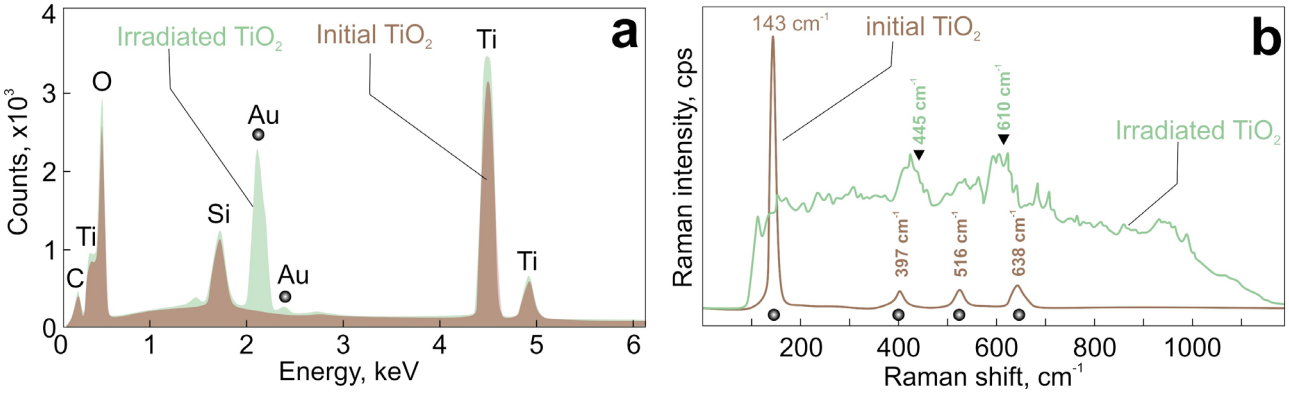

Fig. 2 (a) EDX spectra of the initial (brown) and irradiated (green) TiO_2 nanoparticles indicating the main identified chemical elements. (b) Averaged Raman spectra of the initial (brown) and laser-irradiated (green) TiO_2 nanoparticles. Raman line positions for anatase and rutile marked by circles and triangles, correspondingly.

(marked by circles in Fig. 2b) presented in the Raman spectra of the initial nanomaterial disappear in the Raman signal measured from Au-TiO_2 nanoparticles. Regardless of Au decoration degree the Raman spectra of such hybrid nanoparticles demonstrate a broadband signal with only two low-intensity peaks that presumably associated with rutile inclusions (marked by triangles in Fig. 2b). These inclusions can be located inside the nanoparticle while the outer shell can represent a disordered (amorphous) Ti_2O_3 layer [30,31]. Raman signal of the surface layers is expected to be enhanced by Au nanoparticles, but the observed peaks have a low intensity that is partially confirmed this assumption. The Raman spectra of hybrid nanoparticles measured with different laser sources with wavelengths of 532 and 780 nm did not show significant contrast. A detailed studying the crystalline structure of PLAL-synthesized Au-decorated TiO_2 nanoparticles will become a subject of our forthcoming work.

High RI (n>2) spherical dielectric nanoparticles are known to support magnetic and electric Mie-type resonances [32]. Decoration of such subwavelength resonant structures with plasmon-active noble-metal nanoparticles, whose localized plasmon resonances coincide in frequency with Mie-type resonances, is prospective for advanced light manipulation, sensing, and enhancement of photophysical effects [7,8,33]. To demonstrate the potential of PLAL-synthesized hybrid nanoparticles for listed applications, we measured and analyzed the dark-field scattering spectra of isolated Au-TiO_2 nanostructures with different decoration degree in the visible spectral range. For such measurements, dispersed hybrid nanoparticles were drop-casted on the glass substrate, particle concentration was chosen to enable one the deposition and subsequent analysis of individual nanoobjects.

Fig. 3a represents two dark-field scattering spectra measured from single hybrid nanoparticles of the same diameter (≈610 nm), but significantly different in the decoration degree. The both spectra show a number of coincident features in the visible spectral range which are apparently related to the high-order Mie resonances maintained by the dielectric part of the hybrid nanoparticle (the position of the 1st-order magnetic dipole resonance for a particle of diameter D and refractive index n is determined by ≈D*n). At the same time, a two-fold increase in the dark-field scattering intensity in the red spectral region (550-750 nm) for a strongly decorated particle is associated with the expected contribution from plasmon-induced resonance scattering of gold nanoparticles located on the TiO_2. Red-shifting of scattering band for plasmon-active particles can be explained by their hemispherical shape that provides strong contact with the TiO_2 surface, which has a high refractive index [34]. In addition, interacting electromagnetic fields of gold nanoparticles located closer than 30 nm to each other can also contribute to scattering pattern in this wavelength range.

For Mie-type magnetic resonances, the electromagnetic field is mainly concentrated inside the particle. However, the presence of plasmon nanoclusters on the particle surface allows one to convert part of the radiation “localized” inside the particle for more efficient pumping of plasmon

nanoparticles near-fields. This is clearly illustrated in Fig. 3b,c by comparative numerical calculations of the structure and intensity of electromagnetic fields near all-dielectric (TiO_2) and hybrid (Au-TiO_2)

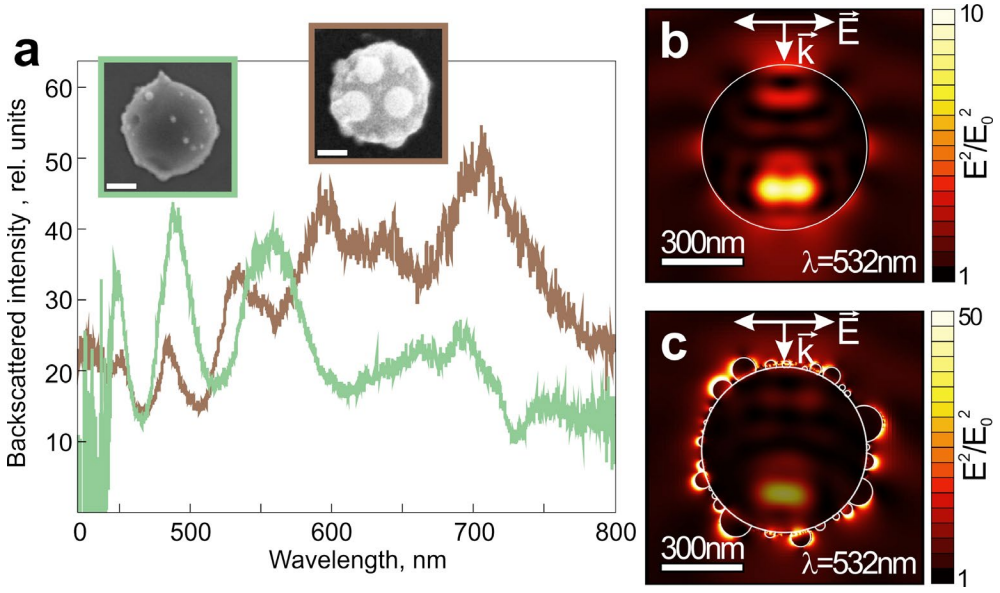

Fig. 3 (a) Dark-field scattering spectra measured from isolated TiO_2 nanoparticles with the same diameter of 610 nm and different decoration degree with gold nanoparticles. The insets show SEM images of the corresponding nanoparticles. (b, c) The calculated normalized electromagnetic field intensity (E^2/ E_0^2) near the surface and inside spherical TiO_2 nanoparticles with the same diameter of 600 nm and different decoration degree. The calculations are given for exciting x-polarized 532-nm wavelength source.

nanoparticles with a diameter of 610 nm. Obviously, the presence of gold nanoparticles causes decrease of Mie-resonance Q-factor which is also observed in the measured scattering spectra of two hybrid nanoparticles outside the plasmon scattering band. Nevertheless, it allows one to achieve a significant electromagnetic field enhancement near the decorating nanoparticles surface at wavelengths coinciding with the Mie resonances position, which is of great importance for a number of practical applications.

Summary

In conclusion, using the simple and high-performance PLAL method, we demonstrated the possibility to synthesize new promising hybrid nanomaterial - amorphous spherical TiO_2 nanoparticles with an average diameter of 250 nm, decorated with gold nanoclusters. The average size and number of Au nanoclusters reduced on the TiO_2 nanoparticle surface was shown to be tuned by varying the initial nanoparticles/$HAuCl_4$ concentration ratio. At the same time, the average size of the initial TiO_2 nanomaterial will expected to determine the diameter of Au-decorated spherical TiO_2 nanoparticles to be PLAL-synthesized. The capability to control the basic geometric parameters of hybrid nanoparticles, that is promising for numerous applications of modern optics, including realization of advanced chemo- and biosensing platforms, as well as of new-generation solar cells, will be studied in detail in our forthcoming works.

Laser-related experiments were supported by Russian Science Foundation (grant no. 19-79-00214). A.K. expresses gratitude to the Ministry of Science and Higher Education of the Russian Federation (grant no. MK-3258.2019.8).

References

[1] S.A. Maier, Plasmonics: fundamentals and applications, Springer Science & Business Media, Berlin, 2007.
[2] A. Kuchmizhak, S. Gurbatov, Yu. Kulchin, O. Vitrik, Plasmon mode excitation and photoluminescence enhancement on silver nanoring, Opt. Comm. 356 (2015) 1.
[3] A. Arbabi, Y. Horie, M. Bagheri, A. Faraon, Dielectric metasurfaces for complete control of phase and polarization with subwavelength spatial resolution and high transmission, Nature Nanotech. 10 (2015) 937.
[4] A. Kuchmizhak, S. Gurbatov, Yu. Kulchin, O. Vitrik, Plasmon mode excitation and photoluminescence enhancement on silver nanoring, Opt. Comm. 356 (2015) 1.
[5] D. Pavlov, S. Syubaev, A. Kuchmizhak, S. Gurbatov, O. Vitrik, E. Modin, S. Kudryashov, X. Wang, S. Juodkazis, M. Lapine, Direct laser printing of tunable IR resonant nanoantenna arrays, App. Surf. Sci. 469 (2019) 514.
[6] Y.H. Fu, A.I. Kuznetsov, A.E. Miroshnichenko, Y.F. Yu, B. Luk'yanchuk, Directional visible light scattering by silicon nanoparticles, Nat. Commun. 4 (2013) 1527.
[7] D.A. Zuev, S.V. Makarov, I.S. Mukhin, V.A. Milichko, S.V. Starikov, I.A. Morozov, I.I. Shishkin, A.E. Krasnok, P.A. Belov, Fabrication of Hybrid Nanostructures via Nanoscale Laser-Induced Reshaping for Advanced Light Manipulation, Adv. Mater. 28 (2016) 3087.
[8] R. Jiang, B. Li, C. Fang, J. Wang, Metal/semiconductor hybrid nanostructures for plasmon-enhanced applications, Adv. Mater. 26 (2014) 5274.
[9] W. Liu, A.E. Miroshnichenko, D.N. Neshev, Y.S. Kivshar, Broadband unidirectional scattering by magneto-electric core–shell nanoparticles, ACS Nano 6 (2012) 5489.
[10] H. Wang, P. Liu, Y. Ke, Y. Su, L. Zhang, N. Xu, S. Deng, H. Chen, Janus magneto–electric nanosphere dimers exhibiting unidirectional visible light scattering and strong electromagnetic field enhancement, ACS Nano 9 (2015) 436.
[11] A. Devilez, B. Stout, N. Bonod, Compact metallo-dielectric optical antenna for ultra-directional and enhanced radiative emission, ACS Nano 4 (2010) 3390.
[12] E. Rusak, I. Staude, M. Decker, J. Sautter, A.E. Miroshnichenko, D.A. Powell, D.N. Neshev, Y.S. Kivshar, Hybrid nanoantennas for directional emission enhancement, Appl. Phys. Lett. 105 (2014) 221109.
[13] T.C. Damato, C.C. de Oliveira, R.A. Ando, P.H. Camargo, A Facile Approach to TiO2 Colloidal Spheres Decorated with Au Nanoparticles Displaying Well-Defined Sizes and Uniform Dispersion, Langmuir 29 (2013) 1642.
[14] S.T. Kochuveedu, D.P. Kim, D.H. Kim, Surface-Plasmon-Induced Visible Light Photocatalytic Activity of TiO_2 Nanospheres Decorated by Au Nanoparticles with Controlled Configuration, J. Phys. Chem. C 116 (2012) 2500.
[15] Y. Wang, H.B. Fang, Y.Z. Zheng, R. Ye, X. Tao, J.F. Chen, Controllable assembly of well-defined monodisperse Au nanoparticles on hierarchical ZnO microspheres for enhanced visible-light-driven photocatalytic and antibacterial activity, Nanoscale 7 (2015) 19118.
[16] R. Ghosh Chaudhuri, S. Paria, Core/shell nanoparticles: classes, properties, synthesis mechanisms, characterization, and applications, Chem. Rev. 112 (2012) 2373.
[17]. D. Zhang, B. Gökce, S. Barcikowski, Laser synthesis and processing of colloids: fundamentals and applications, Chem. Rev. 117 (2017) 3990.
[18] S. Reich, P. Schönfeld, P. Wagener, A. Letzel, S. Ibrahimkutty, B. Gökce, S. Barcikowski, A. Menzel, T. dos Santos Rolo, A. Plech, Pulsed laser ablation in liquids: Impact of the bubble dynamics on particle formation, J. Colloid Interface Sci. 489 (2017) 106.
[19] F. Taccogna, M. Dell'Aglio, M. Rutigliano, G. Valenza, A. De Giacomo, On the growth mechanism of nanoparticles in plasma during pulsed laser ablation in liquids, Plasma Sources Sci. Technol. 26 (2017) 045002.

[20] E.V. Barmina, G.A. Shafeev, Formation of core–shell Fe@Al nanoparticles by laser irradiation of a mixture of colloids in ethanol, Quantum Electron. 48 (2018) 637.
[21] Y. Feng, Z. Li, H. Liu, C. Dong, J. Wang, S.A. Kulinich, X.W. Du, Laser-Prepared CuZn Alloy Catalyst for Selective Electrochemical Reduction of CO_2 to Ethylene, Langmuir 34 (2018) 13544.
[22] M. Honda, T. Goto, T. Owashi, A.G. Rozhin, S. Yamaguchi, T. Ito, S.A. Kulinich, ZnO nanorods prepared via ablation of Zn with millisecond laser in liquid media, Phys. Chem. Chem. Phys. 18 (2016) 23628.
[23] H.B. Zeng, X.W. Du, S.C. Singh, S.A. Kulinich, S.K. Yang, J.P. He, W.P. Cai, Nanomaterials via laser ablation/irradiation in liquid: a review, Adv. Funct. Mater. 22 (2012) 1333.
[24] D.A. Goncharova, T.S. Kharlamova, I.N. Lapin, V.A. Svetlichnyi, Chemical and Morphological Evolution of Copper Nanoparticles Obtained by Pulsed Laser Ablation in Liquid, J. Phys. Chem. C 123 (2019) 21731.
[25] S.A. Kulinich, T. Kondo, Y. Shimizu, T. Ito, Pressure effect on ZnO nanoparticles prepared via laser ablation in water, J. Appl. Phys. 113 (2013) 033509.
[26] N. Mintcheva, P. Srinivasan, J.B.B. Rayappan, A.A. Kuchmizhak, S.O. Gurbatov, S.A. Kulinich, Room-temperature gas sensing of laser-modified anatase TiO_2 decorated with Au nanoparticles, Appl. Surf. Sci. 507 (2020) 145169.
[27] I.N. Saraeva, N. Van Luong, S.I. Kudryashov, A.A. Rudenko, R.A. Khmelnitskiy, A.L. Shakhmin, A.Y. Kharin, A.A. Ionin, D.A. Zayarny, D.H. Tung, P.V. Duong, P.H. Minh, Laser synthesis of colloidal Si@ Au and Si@ Ag nanoparticles in water via plasma-assisted reduction, J. Photochem. Photobiol. A 360 (2018) 125.
[28] P. Liu, H. Chen, H. Wang, J. Yan, Z. Lin, G. Yang, Fabrication of Si/Au core/shell nanoplasmonic structures with ultrasensitive surface-enhanced Raman scattering for monolayer molecule detection, J. Phys. Chem. C 119 (2015) 1234.
[29] C. Rodrigues, J. Bobb, M. John, S. Fisenko, M. El-Shall, K. Tibbetts, Nucleation and growth of gold nanoparticles initiated by nanosecond and femtosecond laser irradiation of aqueous $[AuCl_4]^-$, Phys. Chem. Chem. Phys., 20 (2018) 28465.
[30] M. Tian, M. Mahjouri-Samani, G. Gyula Eres, R. Sachan, M. Yoon, M.F. Chisholm, K. Wang, A.A. Puretzky, C.M. Rouleau, D.B. Geohegan, G. Duscher, Structure and Formation Mechanism of Black TiO_2 Nanoparticles, ACS Nano 9 (2015) 10482.
[31] V.A. Zuñiga-Ibarra, S. Shaji, B. Krishnan, J. Johny, S.S. Kanakkillam, D.A. Avellaneda, J.A. Aguilar Martinez, T.K. Das Roya, N.A. Ramos-Delgado, Synthesis and characterization of black TiO_2 nanoparticles by pulsed laser irradiation in liquid, Appl. Surf. Sci. 483 (2019) 156.
[32] A.I. Kuznetsov, A.E. Miroshnichenko, M.L. Brongersma, Y.S. Kivshar, B. Luk'yanchuk, Optically resonant dielectric nanostructures, Science 354 (2016) 846.
[33] A.O. Larin, A. Nominé, E.I. Ageev, J. Ghanbaja, L.N. Kolotova, S.V. Starikov, S. Bruyère, T. Belmonte, S.V. Makarov, D.A. Zuev, Plasmonic nanosponges filled with silicon for enhanced white light emission, Nanoscale 12 (2020) 1013.
[34] S. Gurbatov, O. Vitrik, Y. Kulchin, A. Kuchmizhak, Mapping the refractive index with single plasmonic nanoantenna, Sci. Rep. 8 (2018) 1.